# Thermal modeling of batteries for EV energy management

Ali Abbas, Nassim Rizoug, Rochdi Trigui, Anthony Babin, Eduardo Redondo-Iglesias, Serge Pelissier

# Thermal modeling of batteries for EV energy management

Ali ABBAS*[1,2], Nassim RIZOUG[1], Rochdi TRIGUI[2], Anthony BABIN[1] , Eduardo REDONDO-IGLESIAS[2], Serge PELISSIER[2]
[1]S2ET, ESTACA, Laval, France
[2]LICIT-ECO7, Gustave Eiffel University, Bron, France
*Corresponding author: ali.abbas@estaca.fr

***Abstract*— The temperature of a Lithium-ion battery was investigated, a 3D modeling approach was adopted. With the assitance of ANSYS Fluent software, the evolution of the temperature was predicted for one cell and then the work has been extended to a module of several cells. It was found for both cases, that the temperature increased when the discharge current increased. Regarding the module, the maximum temperature was achieved by the middle cells. A cooling air system was introduced into the module with different inlet velocities, and it was noticed that the temperature decreased with the increase of the velocity.**

***Keywords—Lithium-ion battery, thermal modeling, multi-scale multi-domain, energy management.***

## I. INTRODUCTION

Due to the growing concerns about environmental issues and energy shortage, the demands for a permanent and long-term transition to a sustainable energy have been increasing in the transport field [1]. In this regard, the automotive sector has renewed its focus on electrification as a solution against all the challenges [2]. In terms of efficiency and pollution reduction during driving phases, electric and hybrid electric vehicles are superior compared to conventional ones [2, 3]. The temperature on which a battery is working is vital when considering the safety and the performance of electric vehicles (EVs). This is why it is crucial to have a prediction of the temperature of the battery. Among available technologies, Lithium-ion batteries are often used for electric vehicles thanks to their energy and power density, high life span, and low self-discharge [4]. However, this technology faces some challenges in terms of cost and safety issues, for instance: danger of explosion in case of overheating. During operation, Lithium-ion batteries are subject to several thermal and electrical conditions, such as operating under different ambient temperatures and driving cycles, which will generate heat and eventually cause energy loss. The heat generated during the functioning time of the battery is mainly caused by two processes: irreversible and reversible heat [5]. Irreversible heat: also referred to as " the heat generated by Joule effect", this type of losses is directly linked to the internal resistance of the cell. Studies have shown that joule effect is responsible of more than half of the total heat generated by the Lithium-ion battery since it varies with the square of the current, this term is always positive [6]. Reversible heat: this term is linked to the entropic coefficient which is the derivative of the open circuit voltage (OCV) over the temperature, and its value can be either positive or negative. An allowable operational temperature for Lithium-ion batteries generally ranges between −20 °C and 60 °C, while temperatures ranging from 15 °C and 35 °C will ensure an optimal performance [7]. It also needs to be mentioned, that keeping a temperature gradient between the cells in the battery pack less than 5°C, will help us increase the lifespan of the battery [8]. This is due to the fact that a large non-uniformity in the temperature all over the pack of the battery will increase the degradation of the cells [9]. It therefore remains vital to develop an efficient thermal management system in order to improve the performance of the battery as an addition to the vehicle. In order to have a better understanding of their behavior under different electric cycles and ranges of temperature, thermal modeling of Lithium-ion cells is required. This procedure will help us reduce the number of tests needed and also to develop an adequate thermal management system of a battery pack. Numerical simulations are considered as one of the most employed methods to model the thermal behavior of the battery under different conditions without having the need each time to apply experiments with specific situations on it. The challenge of a Lithium-ion battery modeling is linked to its multidomain multiphysics nature, several components of the battery coupled with different thermophysical properties make the problem more difficult. The multi-scale multi-domain "MSMD" offers a solution for this physical complexity [10]. Under this approach, several electro-thermal-chemical models have been illustrated in previous studies ranging from empirical models to chemical-based models. Starting with the Newman, Tiedman, Gu and Kim model also referred to as the "NTGK", this is a semi-empirical model suggested firstly by Kwon et al [11]. In this model, the volumetric current is linked to the cell voltage with a linear function, the NTGK model is characterized by two parameters 'U' and 'Y' that can be determined based on data obtained from experimental tests performed on the battery cell (discharge tests under different current rates and temperature range). Secondly, we have the "ECM", known as the electric circuit model, that also uses empirical parameters as input data. In this model, the battery is presented by a circuit composed of resistors and capacitors. Chen [12] adopted a six parameters circuit that includes three resistors and two capacitors which depended on the state of charge of the battery (SOC). However, a curve fitting of the experimental data is needed in order to determine the electrical parameters. Finally, the Newman "P2D" model [13] is a theoretical model that takes into account several physical and chemical processes such as: i) the transfer and the insertion of Lithium-ions to the electrolyte phase and the active electrodes respectively, ii) the electrochemical reaction that occurs during the transfer of the ions. However, P2D is considered as one of the most complicated models compared to others since it requires large number of input parameters and as

a result a long duration of calculation. 3D thermal simulation has also been used in order to study the air-cooling plate system added to the Lithium-ion battery pack. Despite the fact that this system of cooling has been applied in EVs, studies surrounding the evolution of the temperature of the cells resulting from the interaction occurring between the heat generated and the flow of the air inside the cold plates has not been thoroughly analyzed. The present work investigates the thermal behavior of Lithium-ion battery during discharge cycles as a first step. The NTGK model has been used on both single cell and a module of cells in order to estimate the evolution and the distribution of the temperature of the battery cells during the operating phases. One of the benefits of using this model compared to typical electric models is that, along with the effect of the state of charge, or depth of discharge (DOD), on the electrical parameters, an additional temperature dependency on the internal resistance (R[Ω]) and the OCV [V] that is based on the principles of the Seebeck effect and the Arrhenius equation of chemical kinetics, has thus been included [14]. This will help in improving the accuracy in the determination of the heat generated inside the battery cell. By doing so, this accuracy in measuring the internal heat will in turn allow us, through the energy equation implemented in the model, to have a precise measurement of the battery temperature. An examination is performed in order to study the impact of the implementation of the cooling system on the evolution of the maximum temperature achieved using 3D thermal modeling. The paper is structured as such: Section II depicts the modeling procedure and is divided as follows: i) the design and parameterization of the battery cell, ii) the model methodology and formulation. As for Section III, this part illustrates the results of the simulation for one single cell, a module of battery, and the effect of the air-cooling system proposed for the module on the temperature. Conclusions are given in Section IV.

## II. MODELING PROCEDURE

### A. *Design and parameterization*

The Lithium-ion battery cell studied is a pouch cell having a nominal capacity of 14.6 Ah and composed of $LiMn_2O_4$ as the cathode material and graphite as the anode material, the positive current collector is made of aluminum while the negative one is made of copper. The reason this technology of battery was chosen, is due to its life span which is lower compared to other types [15], thus an accurate thermal modeling of this battery is required in order to develop an effective thermal management system, capable of maintaining its functioning temperature in optimal range whilst extending its life span. The work started by modeling the thermal performance of one single cell during discharge cycles at different C-rates, then it was extended to a module composed of several cells connected in series. As mentioned previously, the modeling of Lithium-ion battery is difficult because of the multi-physics nature of the cell. The MSMD approach was found to face this challenge with the assumption of considering the active cell as a homogenous body and by that it means an equivalent material that is a combination of the different layers as illustrated in Fig. 1. As a result, the geometry of the Lithium-ion cell in the simulation is composed of three solid bodies. Two bodies that represent the positive and negative tabs, and the third one is the active cell which is composed of five layers, the positive and negative electrodes and current collectors, and the separator that prevents the insertion of the ions directly from the electrode to the other. The components of the equivalent active material in the thickness direction, z-axis, as well as the dimensions of the three solid bodies with the units in mm are shown in Fig. 1. In the case of a module, we have to add a new solid " Busbar" in order to connect the cells to each other. The geometry of the solid parts was created using the design software SOLIDWORKS, and the bodies were then imported into the software ANSYS Fluent, where we performed the meshing of the different domains in order to start with the simulation. The thermal and physical parameters of the active cell were calculated based on the components already mentioned and by using the following equations [16]:

$$\lambda_{x,y} = \frac{\sum_{i=1}^{5} \lambda_i L_i}{\sum_{i=1}^{5} L_i} \quad (1)$$

$$\lambda_z = \frac{\sum_{i=1}^{5} L_i}{\sum_{i=1}^{5} \frac{L_i}{\lambda_i}} \quad (2)$$

$$C_p = \frac{\sum_{i=1}^{5} C_{p_i} L_i}{L_{cell}} \quad (3)$$

$$\rho = \frac{M_{cell}}{V_{cell}} \quad (4)$$

Where λ [W/K.m], Cp[J/K.Kg], ρ[Kg/m$^3$] and L[m] represent the thermal conductivity, the specific heat capacity, the density, and the thickness of the materials respectively, $V_{cell}$ [m$^3$] and $M_{cell}$ [Kg] denote the volume and the mass of the active cell respectively, the index 'i' refers to the component of the cell. The parameters of the layers composing the Lithium-ion cell were taken from the literature [14]. Regarding the equivalent thermal conductivity, it was calculated based on the parallel-series configuration, in the x and y axis, parallel configuration, this parameter was estimated with respect to (1), while it was calculatd based on (2) in the z-direction (series).

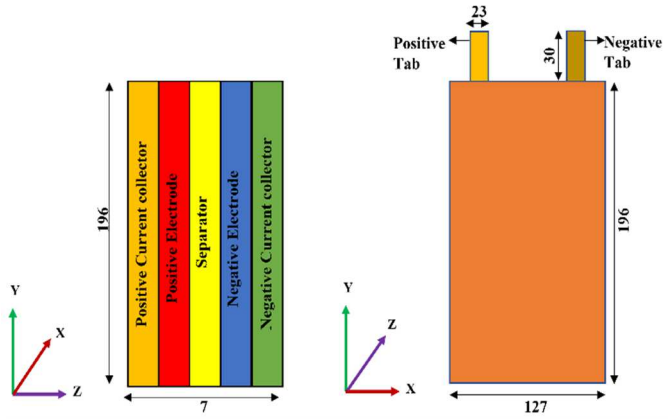


Fig. 1. Components of the active cell in the z direction (thickness direction) and the dimensions of the three solid bodies (units in mm)

### B. *MSMD and NTGK formulation*

The methodology of the battery modeling using the "NTGK" is illustrated in Fig. 2, where the suggested model uses several input data, such as the thermal and electrical conditions on which the battery is operating, add to that also the physical parameters of the battery, in order to estimate the heat generated inside the

cell, and the evolution of the temperature with the help of the coupling done between both the thermal and the electrical fields.

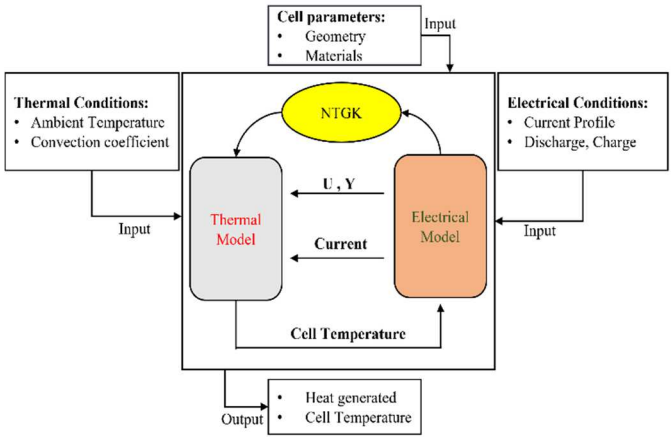


Fig. 2. Illustration of the Lithium-ion modeling using the NTGK model

The estimation of the internal heat and the temperature is done based on three equations [17]: the energy balance equation (5), and the poisson equations (6,7).

$$\rho C_p \frac{\partial T}{\partial t} = \nabla(\lambda \nabla T) + \sigma_+(\nabla \phi_+)^2 + \sigma_-(\nabla \phi_-)^2 + q_{ech} \quad (5)$$

$$\nabla.(\sigma_+ \nabla \phi_+) = -J_{ech} \quad (6)$$

$$\nabla.(\sigma_- \nabla \phi_-) = J_{ech} \quad (7)$$

Where σ [S/m] and $\phi$ [v] represent the electric conductivity and the potential of the two electrodes respectively, and the term $J_{ech}$ [$A/m^3$] represents the volumetric current and can be expressed as function of the voltage of the cell, which is the difference between the potentials of the two electrodes, as shown in the following equation:

$$J_{ech} = \frac{C_{nom}}{C_{ref} V_{cell}} Y[U - (\phi_+ - \phi_-)] \quad (8)$$

Where Y [S], denotes the electrical conductance (the reciprocal of the internal resistance of the cell), is the inverse of the slope of the voltage-current curve, and U [v], which represents the open circuit voltage (OCV), is the intersection between the V-I curve and the voltage axis [18], both Y and U illustrate the functional parameters of the NTGK model, $C_{nom}$ represents the nominal capacity of the cell, and $C_{ref}$ represents the reference capacity at which the battery has been tested in order to determine Y and U. Equation (8) is inspired by Gu [18], who in order to estimate the two parameters already mentioned, performed discharging cycles on a cell periodically until the voltage reached its cutoff limit and a polynomial relationship between the NTGK parameters and the depth of discharge has been established in (9) and (10):

$$U = \sum_{j=0}^{N} a_j \, DOD^j \quad (9)$$

$$Y = \sum_{j=0}^{N} b_j \, DOD^j \quad (10)$$

The coefficients $a_j$ and $b_j$ shown above are constants to be fitted based on voltage-current curves obtained during the experiments done. In order to take into account the impact of the temperature on the functional parameters of the model, the equations listed previously were reformulated by Kim [14]:

$$U = U_0 - C_1(T_i - T_{ref}) \quad (11)$$

$$Y = Y_0 \exp[-C_2(\frac{1}{T_i} - \frac{1}{T_{ref}})] \quad (12)$$

Where $U_0$ and $Y_0$ represent the values of U and Y at a reference temperature $T_{ref}$ [K], which is also the ambient temperature, as for $T_i$ [K] this term represents the temperature of the battery cell. $C_1$ and $C_2$ are the NTGK constants for a specific battery cell that are required to fit the temperature dependency on Y and U and are determined based on the Arrhenius and Nernst equations [19]. And finally regarding the last two terms on the right of (5), we have the first one that represents the ohmic heating, while the second term is the electrochemical volumetric heat source generated inside the battery cell $q_{ech}$ [$W/m^3$], which is the sum of the irreversible and reversible term as shown in (13), where the irreversible heat is expressed as the volumetric current multplied by the difference between the OCV and the voltage of the cell, and the reversible heat part is equal to the volumetric current multiplied by the internal temperature of the cell and the entropic heat coefficient:

$$q_{ech} = J_{ech}[(U - (\phi_+ - \phi_-)) - T_i \frac{dOCV}{dT}] \quad (13)$$

It is also important to mention, that the face of the cell that is directly exposed to the environment, is subject to convection heat transfer mode. Due to this type of heat transfer, the heat generated inside the cell will be dissipated into the atmosphere since the ambient temperature might be lower than the surface temperature of the cell that is in contact with the atmosphere. In this case, we have to define the rate of the convection heat transfer with the following equation:

$$Q = h.A(T_s - T_{amb}) \quad (14)$$

Where A [$m^2$] represents the area at which the convection heat transfer is occurring, $T_s$ [K] and $T_{amb}$ [K] are the surface and the ambient temperature respectively, while h [$W/K.m^2$] denotes the convection heat transfer coefficient. In the case of a module, in addition to the thermal equations already listed, we have to take into account the gaps between the cells, which were considered as confined spaces and filled with air. In order to determine the heat transfer mode happening between the cells, a dimensionless parameter, called the Rayleigh number which is the product of Grashof and Prandtl number, also dimensionless parameters, is used [20] and expressed as follows:

$$R_a = \frac{g\beta(T_1 - T_2)e^3}{\alpha_a \upsilon} \quad (15)$$

Where e[m] represents the thickness of the gap between the cells, $(T_1-T_2)$ [K] is the temperature difference between the gap walls, g [$m/s^2$] is the acceleration due to earth's gravity, β[1/K] is the thermal expansion coefficient, υ[$m^2/s$] and $\alpha_a$ [$m^2/s$] denote the kinematic viscosity and the thermal diffusivity of the air respectively. At a range of values of Rayleigh number lower than threshold Rayleigh's number of the air, heat transfer takes place by conduction through the air gaps. In our situation, since the distance between the cells is very small, 2mm, the Rayleigh number is thus less than 1000. Hence, the heat transfer through the air in the gaps happens by conduction. In this study, the gaps were modeled as solid domains during the simulation with the thermal and physical properties of the air.

## III. Results

### A. One single cell

The work started by modeling the thermal behavior of one single cell at four different discharge current rates (1C, 3C, 5C, and 10C) until the cell is fully discharged. The initial depth of discharge was set to 0 since the simulation of the battery is done during discharge phases. The constant coefficients in (9) and (10) previously estimated were used. In the Fluent Framework, the solid cell body was selected as an active zone, while the positive and negative solid tabs were assigned as passive zones. Concerning the thermal boundary properties of the cell and the tabs, a natural heat convection transfer mode was considered with a coefficient of convection value equal to 5 [21], and the temperature of the atmosphere in which the battery is located was set to 300 K, that is equivalent to 27°C. The simulation stopped once the cell has reached its discharge voltage limit. Fig. 3 depicts the evolution of the voltage of the cell during the different discharge cycles, and as it is noticed the cut-off voltage limit was achieved faster with higher discharge rates applied. It took 3440 seconds to completely discharge the cell at 1C, while this value decreased to 360 seconds at a C-rate of 10. The small difference between the values of the voltage at the end of each discharge cycle is due to the step size, set to 1 second during the simulation, which has caused this small discrepancy. It is also important to mention that in reality the computation time of the simulation was almost 3060 seconds for the case of one single cell during a discharge cycle of 10C, while this value increased during simulations at lower C-rates, for instance it took almost 29200 seconds in order to finish a 1C discharge phase simulation. Noteworthy, that the computation time of the simulation of the module of battery will also increase compared to one single cell case, since we have to take into consideration the element size chosen for the meshing procedure and the number of the solid domains modeled, such as the cells, busbars, tabs, and the gaps between the cells. The duration of the simulation will also increase with the implementation of the cooling system.

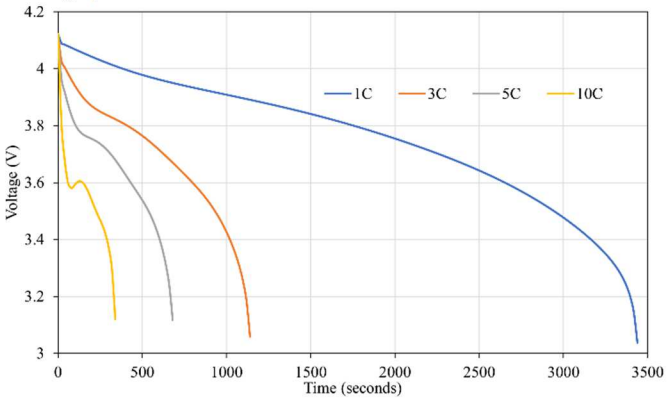


Fig. 3. Evolution of the voltage of the cell during 4 different discharge rates

The evolution of the maximum temperature achieved during the four discharge cycles is illustrated in Fig. 4, and as it is shown, the temperature of the cell has been increasing each time the discharge current rate increased. A maximum temperature achieved during a 1C-rate discharge cycle was 30°C, while this temperature increased to 42°C, 52°C and 77.6°C at discharge rates of 3C, 5C and 10C respectively.

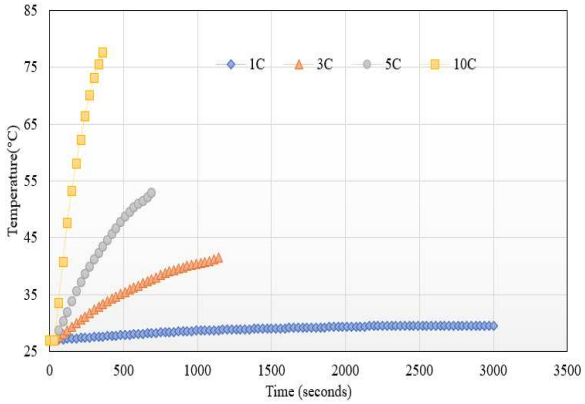


Fig. 4. Evolution of the maximum temperature of a cell during four different discharge rates

### B. Module of battery

Other simulations were done for several cells connected in series. The procedure in the case of a module is similar to the previous one. Same thermal conditions as the "one single cell" case, regarding the coefficient of convection and the ambient temperature, were applied. The volume of the air gaps between the cells has been taken into consideration in ANSYS Fluent and modeled. A first study was done regarding the impact of the discharge current applied on the module, and it was noticed that the temperature also has been increasing with the increase of the discharge current rate applied. A second study was done in order to investigate the effect of the number of the cells on the thermal behavior of the battery module. The module was composed of several cells connected in series, ranging from two to ten cells, and a comparison was established in terms of the maximum temperature achieved during a 10C-rate discharge cycle. The reason this value of current rate was chosen is because according to the simulation, at this rate the battery has been achieving high temperatures compared to the normal ranges of temperature of Lithium-ion battery, which might lead eventually to an increase in the risk of the thermal runaway or at least a premature aging of the battery, an air-cooling plate system is proposed later on in order to examine its effect on the evolution of the temperature during the 10C discharge phase. The graph in Fig. 5 illustrates a comparison of the maximum temperature obtained by each cell of different battery modules during a discharge cycle of 10C. A rise of almost 3°C is noticed for the maximum temperature achieved for a module composed of two cells compared to one cell. This value of temperature has been increasing in the simulation each time the number of cells implemented inside the module has increased. A symmetrical profile of the temperature can be also seen in the case of a module composed of three cells and above, and concerning the internal cells located in the middle of the module, they have been achieving higher temperature compared to those exposed to the air, which are located on the outside of the module. The maximum temperature achieved by the module has been rising with the increasing of the number of cells.

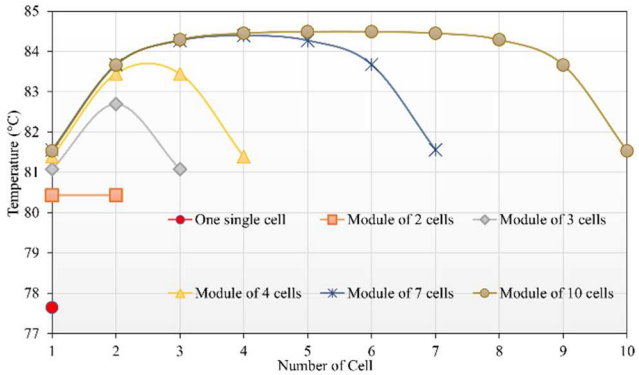


Fig. 5. Comparison of the maximum temperature achieved by each cell of different battery modules

The distribution of the temperature at the end of the discharge cycle of 10C-rate for a module composed of ten cells and four cells connected in series is shown in Fig. 6, left and right side respectively. As it is seen, this contour shows clearly how the heat is mainly accumulated in the middle of the cells and the module.

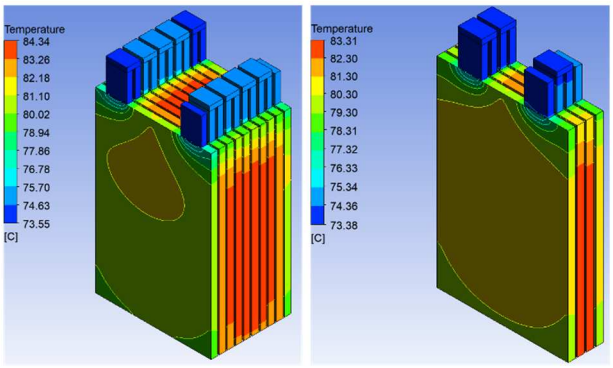


Fig. 6. Contour of temperature at the end of discharge cycle of 10C for a module of 10 cells (on the left) and module of four cells (on the right)

To make things clearer, Fig. 7 illustrates the contour of the distribution of the temperature for two cells of the module composed of four cells shown in Fig. 6 right side, one of the cells is located on the outside and is directly exposed to the ambient air (Fig. 7 left), while the other is located in the middle of the module (Fig. 7 right). In fact, we presented only two cells instead of four, since according to the results presented in Fig. 5 and Fig. 6, symmetrical profile of the temperature was seen for the module composed of four cells. Thus, the two external cells have identical behavior in terms of temperature distribution, and maximum temperature achieved, same hypothesis can be adopted for the two internal cells located in the middle of the module. We can notice from the contour of temperature in Fig. 7, that the internal cell is heating more than the one that is in contact with the ambient air, which can be explained by the fact that the surface exposed to the air is bigger for the cells on the outside than the cells on the inside of the module. As a result, convection heat transfer mode will occur at the surface of the external cells, and the heat generated inside the external cells will be dissipated in a higher manner compared to the ones in the middle, where according to Rayleigh, a conduction heat transfer mode has occurred in the gaps between the cells. A difference of almost 2.5°C is noticed between the two cells.

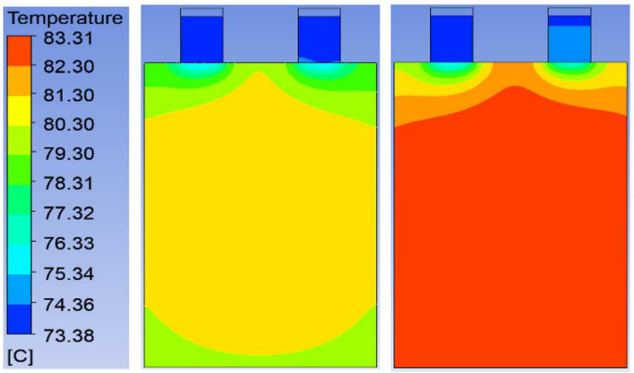


Fig. 7. Contour of the temperature of the external cell (on the left) and internal cell (on the right)

## C. *Integration of cooling system*

As seen previously, the temperature of a module of Lithium-ion battery achieved high values at high C-rates, in our case at 10C, which requires a cooling system to decrease this value. In this part, a cooling method was suggested in order to examine its impact on the maximum temperature achieved by the module composed of four cells already presented in Fig. 6 right. Each cell was surrounded by two air plates that were designed as solid bodies in SOLIDWORKS and then imported into ANSYS Fluent and simulated as fluid regions. The plates were supposed to be identical and have same dimensions as the cell in terms of height and length. The direction of the airflow was supposed to be in the direction of the x- axis. The illustration of the module with the cells surrounded by cooling air plates, and the direction of the air flow passing through the cooling channels are shown in Fig. 8, left and right side respectively. The passive zones in Fig. 8 are represented as follows: red color for the positive tabs, yellow for the negative ones and the busbars are identified with blue color. As for the cells and the cooling plates, they are identified with brown and green colors respectively, regarding the direction of the air flow passing through the air plates, it is represented with yellow color. The simulations were done during a discharge cycle of 10C.

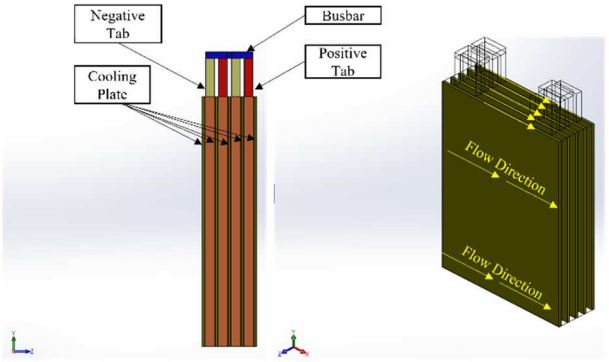


Fig. 8. Illustration of the module of four cells with the cooling plates and the airflow direction

In order to see the influence of the airflow added on the maximum temperature, the examination was done on several inlet velocities. Fig. 9 shows the evolution of the maximum temperature of a module composed of four cells during eight different cooling cases compared to the case without cooling. As

it is illustrated, the maximum temperature decreased when a cooling system was introduced into the module with the help of the cold plates. This temperature also has reduced whenever the inlet velocity of the air increased. While during the case with no cooling system the maximum temperature of the module during a discharge cycle of 10C achieved 83°C at the end of this cycle, this temperature decreased to 76°C, 65°C, and 61°C with a velocity of 1 m/s, 3 m/s, and 4 m/s respectively.

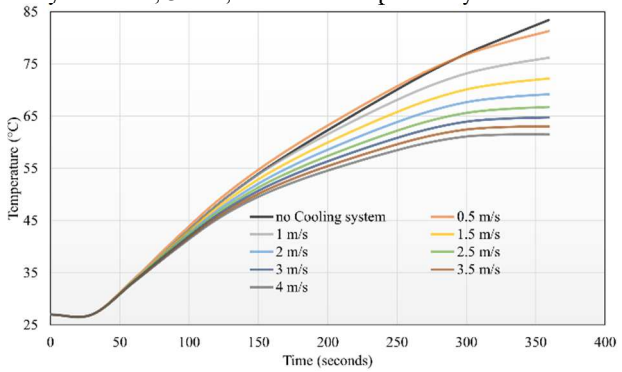


Fig. 9. Evolution of the maximum temperature of a module of four cells during different cooling cases

The graph in Fig. 10 illustrates the value of the maximum temperature achieved by the module for each air inlet velocity, a sharp decrease can be noticed for the value of the temperature when the airflow speed increased from 0 to 2 m/s, with a decrease of almost 14°C. However, above 2 m/s, the temperature started to decrease slowly, dropping 4.4°C when the velocity of the air increased from 2 to 3 m/s. Afterwards, the temperature decreased proportionally to the airflow speed increase, to reach a value of 54°C at 8 m/s.

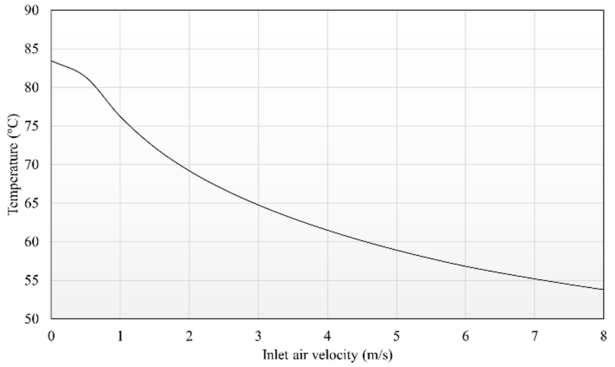


Fig. 10. Evolution of the maximum temperature with the inlet velocities

## IV. Conclusion

In this paper, the thermal performance of a pouch Lithium-ion battery has been investigated. The "MSMD" approach was adopted in this simulation, with the sub-model "NTGK". The first study was done on a single battery cell during four different discharge cycles, where we noticed that the temperature has been increasing with the increase of the C-rate applied, highest temperature has been achieved during discharge current rate of 10. The work has been extended to a module composed of several cells, where we also noticed that the temperature of the module increased with the number of cells. Regarding the cases of three cells and above, a symmetrical profile of the temperature was noticeable with the external cells having lower temperature compared to the cells located in the middle, the heat is mostly accumulated in the middle of the module. In order to reduce the maximum temperature achieved by a module of four cells, an air-cooling system was implemented, with the help of cold plates surrounding each cell, in which several inlet velocities of the air flow were identified. We have seen that the temperature has been decreasing each time we have been increasing the inlet velocity. These results are preliminary work for a study of energy management in EVs. In the future work, the models presented here will be reduced into simpler and faster models. After validation with experiments, they will be then used in the optimal energy and the thermal management of autonomous shared electric vehicles while taking into consideration the battery aging criterion.

## References


[1] M. Ehsani, Y. Gao, A. Emadi, Modern Electric, Hybrid Electric, and Fuel Cell Vehicles: Fundamentals, Theory, and Design, second ed., CRC Press, 2009.

[2] D. Howell, Annual Progress Report for Energy Storage R&D, Vehicle Technologies Program, Energy Efficiency and Renewable Energy, Washington, DC, 2011.

[3] S. Dhameja, Electric Vehicle Battery Systems, Butterworth-Heinemann, 2002.

[4] Yan, Bo, Cheolwoong Lim, Leilei Yin, and Likun Zhu. "Simulation of heat generation in a reconstructed LiCoO2 cathode during galvanostatic discharge" , Electrochimica Acta, 2013.

[5] D. Bernardi, E. Pawlikowski, J. Newman, J. Electrochem. Soc.132 (1985) 5–12.

[6] Zhang, X.Thermal analysis of a cylindrical lithium-ion battery. Electrochim. Acta 2011, 56, 1246–1255.

[7] Yiqun Liu, Y. Gene Liao and Ming-Chia Lai, Transient Temperature Distributions on Lithium-Ion Polymer SLI Battery.

[8] C.-W. Park, A.K. Jaura, Dynamic Thermal Model of Li-Ion Battery for Predictive Behavior in Hybrid and Fuel Cell Vehicles, SAE International, 2003, 2003-01- 2286.

[9] Yang, T.; Yang, N.; Zhang, X.; Li, G. Investigation of the thermal performance of axial-flow air cooling for the lithium-ion battery pack. Int. J. Therm. Sci. 2016, 108, 132–144.

[10] G.H. Kim, K. Smith, K.J. Lee, S. Santhanagopalan, A. Pesaran, Multi-domain modeling of lithium-ion batteries encompassing multi-physics in varied length scales, J. Electrochem. Soc. 158 (2011) A955–A969.

[11] K.H. Kwon, C.B. Shin, T.H. Kang, C.S. Kim, A two-dimensional modeling of a lithium-polymer battery, J. Power Sources 163 (2006) 151–157.

[12] M. Chen, G.A. Rincon-Mora, Accurate electrical battery model capable of predicting runtime and IV performance, IEEE Trans. Energy Convers. 21 (2006) 504–511.

[13] A. aqJokar, B. Retablo, M. Desilts, M. Lacroix, Review of simplified Pseudo-Two-Dimensional models of lithium-ion batteries, J. Power Sources 327 (2016) 44–55.

[14] U. S. Kim et al. "Modeling the Dependence of the Discharge Behavior of a Lithium-Ion Battery on the Environmental Temperature". J. of Electrochemical Soc. 158 (5). A611-A618. 2011.

[15] Y. Miao, P. Hynan, A. von Jouanne, A. Yokochi, Current Li-Ion Battery Technologies in Electric Vehicles and Opportunities for Advancements.

[16] S.C. Chen, C.C. Wan, Y.Y. Wang, Thermal analysis of lithium-ion batteries.

[17] ANSYS Fluent Manual, Modeling Batteries.

[18] H. Gu Mathematical Analysis of a Zn/NiOOH Cell General Motors Research Laboratory, Electrochemistry Department, Warren, Michigan 48090.

[19] A.J. Bard, L.R. Falkner, Electrochemical Methods: Fundamentals and Applications, second ed., John Wiley and Sons, Inc., New York, 2001.

[20] Jack Philip Holman, Heat transfer, 6th ed, New York McGraw-Hill Book Co., 1986.

[21] Philip Kosky, Robert Balmer, William Keat, George Wise, Chapter 12 - Mechanical Engineering.